

## Characterization of effective masses in strained quantum-well laser structures

T. A. Ma and M. S. Wartak

*Department of Physics and Computing, Wilfrid Laurier University, Waterloo, Ontario, Canada N2L 3C5*

(Received 20 June 1994)

Valence-band structures and hole effective masses for strained-layer quantum-well laser structures were calculated, using  $\text{In}_{1-x}\text{Ga}_x\text{As}/\text{InGaAsP}$  material system as an example. A  $4 \times 4$  strain Hamiltonian with heavy-hole and light-hole band mixing was used in the calculation. Systematic numerical results have been presented for a large range of material parameters and quantum-well widths.

### I. INTRODUCTION

In recent years considerable theoretical efforts have been devoted to the analysis of band structures of two-dimensional systems with inclusion of the effect of strain.<sup>1-4</sup> Strain structure consists of thin-layer film which is lattice mismatched to the substrate. This fact produces a uniform elastic strain in the film layer which changes its symmetry with respect to substrate and modifies its electronic and optical properties. Under a compressive strain the heavy-hole band is raised above the light hole, whereas a tensile strain pushes a light hole above the heavy hole.

The efforts were mostly motivated by enormous potential applications of strained-layer structures in optoelectronic industry. In particular, it has been demonstrated that in the case of quantum-well lasers, optical gain, differential gain, and threshold current can be significantly improved by strain. Hole effective masses are among the important parameters needed to properly characterize any particular device. Despite several recent efforts<sup>5-8</sup> the complete picture on hole effective masses is far from clear. The limited experimental results presented in Ref. 6 indicate a strong dependence of the in-plane effective masses of the heavy-hole and light-hole valence bands in quantum wells on their coupling. In general, the band mixing effect posts a much larger challenge in determining hole effective masses than electron effective masses in the conduction band. Negative effective masses at zone center can be predicted in some cases involving band mixing.

The systematic understanding of hole effective masses would also provide a clear picture for the rather complicated strained quantum-well laser designs. This paper is an effort to characterize hole effective masses and quantum-well subbands systematically using  $\text{In}_{1-x}\text{Ga}_x\text{As}/\text{InGaAsP}$  material system.

### II. THEORY

Based on the Luttinger-Kohn Hamiltonian, the total Hamiltonian describing hole energies in the valence band in a quantum well under small uniaxial strain can be expressed as<sup>9,14</sup>

$$H = H_{\text{LK}} + H_{\epsilon}, \quad (2.1)$$

where  $H_{\text{LK}}$  is the Luttinger-Kohn Hamiltonian and  $H_{\epsilon}$  represents the strain Hamiltonian,<sup>14</sup>

$$-H_{\text{LK}} = \frac{\hbar^2}{m_0} \left( \frac{1}{2} \gamma_1 K^2 - \gamma_2 [(J_x^2 - \frac{1}{3} J^2) k_x^2 + \text{c.p.}] - 2\gamma_3 (\{J_x, J_y\} k_x k_y + \text{c.p.}) \right) + V_h(z), \quad (2.2)$$

$$H_{\epsilon} = D_d (\epsilon_{xx} + \epsilon_{yy} + \epsilon_{zz}) + \frac{2}{3} D_u [(J_x^2 - \frac{1}{3} J^2) \epsilon_{xx} + \text{c.p.}] + \frac{4}{3} D'_u (\{J_x, J_y\} \epsilon_{xy} + \text{c.p.}), \quad (2.3)$$

where  $m_0$  is the free-electron mass,  $D_d$ ,  $D_u$ , and  $D'_u$  are deformation energies for valance bands,  $\epsilon_{ij}$  are components of the strain tensor,  $J_i$  are the angular momentum matrices, c.p. indicates cyclic permutation of indices, and  $\{a, b\} = \frac{1}{2}(ab + ba)$ . In spin  $J = \frac{3}{2}$  basis and considering only heavy-hole and light-hole bands, a  $4 \times 4$  Hamiltonian can be derived as

$$H = -\frac{\hbar^2}{2m_0} \begin{pmatrix} P+Q & -S & R & 0 \\ -S^* & P-Q & 0 & R \\ R^* & 0 & P-Q & S \\ 0 & R^* & S^* & P+Q \end{pmatrix} \quad (2.4)$$

with the following definitions:

$$P \pm Q = A_{\pm} + \Gamma_{\pm} k_z^2 + \frac{2m_0}{\hbar^2} V_h(z),$$

$$S = 2\sqrt{3} \gamma_3 (k_x - ik_y) k_z,$$

$$R = -\sqrt{3} \gamma_2 (k_x^2 - k_y^2) + i2\sqrt{3} \gamma_3 k_x k_y,$$

$$A_{\pm} = (\gamma_1 \pm \gamma_2) (k_x^2 + k_y^2) - \frac{2m_0}{\hbar^2} D_d (\epsilon_{xx} + \epsilon_{yy} + \epsilon_{zz})$$

$$\pm \frac{2m_0}{\hbar^2} \frac{1}{3} D_u (\epsilon_{xx} + \epsilon_{yy} - 2\epsilon_{zz}),$$

$$\Gamma_{\pm} = \gamma_1 \pm \gamma_2.$$

In the above,  $\epsilon$  is the strain factor and is defined as  $\epsilon = [a_0 - a(x)/a_0] = \epsilon_{xx} = \epsilon_{yy}$ . For [100] orientation,  $\epsilon_{zz} = -(2C_{12}/C_{11})\epsilon$ , and also  $\epsilon_{xy} = \epsilon_{yz} = \epsilon_{zx} = 0$ .

The discussed approach has its own limitations as has been explained in a series of papers by Burt.<sup>10-13</sup> He has reviewed assumptions of conventional effective-mass theory and had developed a method of handling abrupt interfaces.

The above  $4 \times 4$  Hamiltonian can be block diagonalized into two equivalent  $2 \times 2$  Hamiltonians, which made the calculation fast and easy to use,<sup>14-16</sup>

$$H = -\frac{\hbar^2}{2m_0} \begin{pmatrix} P+Q & |R| - i|S| \\ |R| + i|S| & P-Q \end{pmatrix}. \quad (2.5)$$

The above Hamiltonian can be solved together with the following boundary conditions:

$$\begin{bmatrix} u \frac{\partial}{\partial z} & s \\ -s & w \frac{\partial}{\partial z} \end{bmatrix} \begin{bmatrix} \psi_a(z) \\ \psi_b(z) \end{bmatrix} = \text{continuous}, \quad (2.6)$$

$$\begin{bmatrix} \psi_a(z) \\ \psi_b(z) \end{bmatrix} = \text{continuous}, \quad (2.7)$$

where

$$u = \frac{\hbar^2}{2m_0}(\gamma_1 - 2\gamma_2), \quad w = \frac{\hbar^2}{2m_0}(\gamma_1 + 2\gamma_2),$$

$$s = \frac{\hbar^2}{2m_0} \sqrt{3}\gamma_3 k_x,$$

and  $\psi_a(z)$  and  $\psi_b(z)$  are wave functions.

Figure 1 shows the typical valence-band structures calculated using the method mentioned above for  $\text{In}_{1-x}\text{Ga}_x\text{As}/\text{InGaAsP}$  material system lattice matched to  $\text{InP}$  at  $x=0.37$  which is compressively strained. When calculating effective masses, axial approximation was assumed, i.e., we assume effective masses are isotropic along direction parallel to the surface. In-plane effective masses were calculated from the second-order derivative of subband diagram ( $E-k_{\parallel}$  relations) at zone center.

### III. RESULTS AND DISCUSSION

The lowest band usually dominates device performance. For example, in semiconductor quantum-well lasers, the lowest subband usually has the biggest contribution to optical gain and polarization.<sup>17</sup> TE mode usually dominates when the heavy-hole band is the lowest subband. TM mode usually dominates when the light-hole band is the lowest band. Therefore we would like to focus on the effective masses of the lowest subband. The lowest subband can be determined from Fig. 2 which shows the splitting between the first heavy-hole band and

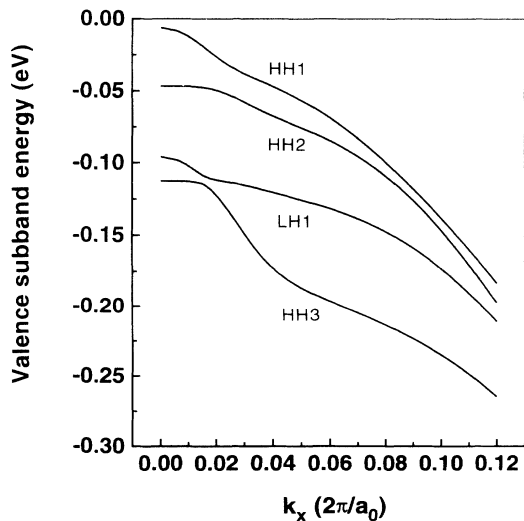


FIG. 1. Valence-band structure for  $\text{In}_{0.63}\text{Ga}_{0.37}\text{As}/\text{InGaAsP}$  quantum well with  $1.25Q$  barrier lattice matched to  $\text{InP}$ .  $L_z=80 \text{ \AA}$ .

the first light-hole band. Positive splitting means the heavy-hole band is the lowest band; on the other hand, negative splitting means the light-hole band is the lowest band. The well width is  $500 \text{ \AA}$  for the lowest curve which can be considered a bulk limit. We can see from Fig. 2 that in the case of compressive strain ( $x < 0.47$ ), the heavy-hole band is always the lowest subband. In the case of tensile strain, the light hole is the lowest subband when well width is sufficiently large. At an  $x$  value above 0.47 (tensile strain), there is a possibility of degeneracy between heavy-hole and light-hole bands as in unstrained bulk material. This is also a transition point where the heavy-hole band and light-hole band exchange relative positions. Band mixing is very strong at this point. Singularities in effective masses usually occur at these transition points which often leads to negative effective masses at zone center.

Figure 3 shows the results of heavy-hole effective masses in strained quantum well as a function of well width for different Ga mole fraction for compressively strained and unstrained cases for  $\text{In}_{1-x}\text{Ga}_x\text{As}/\text{InGaAsP}$  material system. Reduction in effective masses due to compressive strain is very clear (compressive strain becomes larger when  $x$  becomes smaller). Heavy-hole effective masses are also reduced as the well width becomes larger. With the well width increasing, effective masses approach a constant value. Since there are no transition points as defined above, there are no singular points and negative effective masses. The curves are stable and monotonic.

Figure 4 shows the results of light-hole effective masses in strained quantum well as a function of well width for different Ga mole fraction for tensile strain cases in  $\text{In}_{1-x}\text{Ga}_x\text{As}/\text{InGaAsP}$  material system. Reduction in effective masses due to tensile strain is also very obvious, especially with small well width (tensile strain becomes larger as the  $x$  value becomes larger). For each curve in

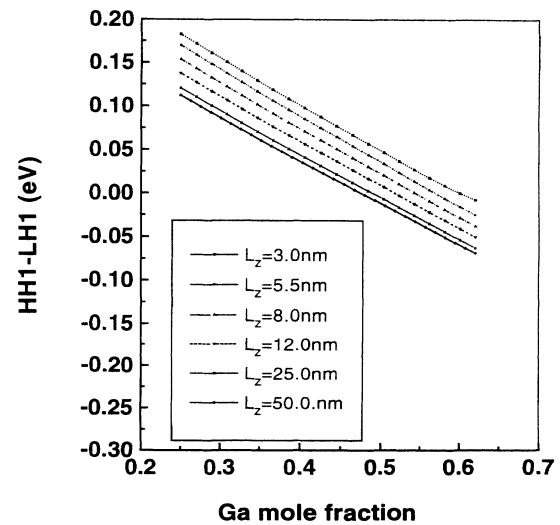


FIG. 2. The difference between the lowest heavy-hole and light-hole subbands in a strained quantum well as a function of well width and Ga mole fraction for  $\text{In}_{1-x}\text{Ga}_x\text{As}/\text{InGaAsP}$  material system.

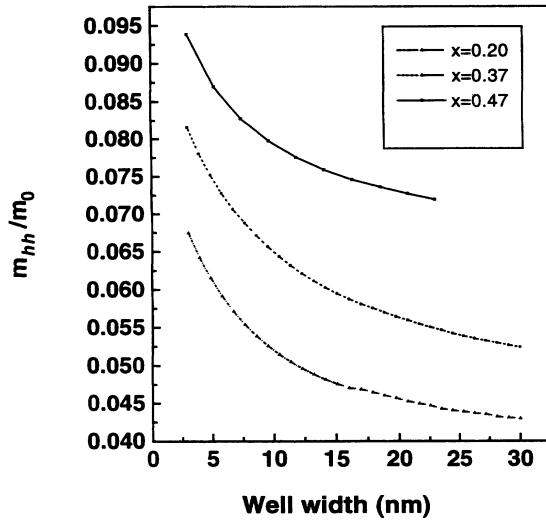


FIG. 3. Heavy-hole effective masses in a strained quantum well as a function of well width for different Ga mole fractions for compressively strained cases in  $\text{In}_{1-x}\text{Ga}_x\text{As}/\text{InGaAsP}$  material system.

Fig. 4, a singular point exists where the calculated effective masses become infinity (it will be negative infinity if approached from the right-hand side). This singularity corresponds to the point where the light-hole subband ceases to be the lowest subband as mentioned before, and the band curvature at zone center changes from positive to negative.

Figure 5 shows the results of heavy-hole effective masses in a strained quantum well as a function of Ga mole fraction for different well width for  $\text{In}_{1-x}\text{Ga}_x\text{As}/\text{InGaAsP}$  material system. Clearly, effective masses are decreasing as strain increases. Again for each curve in Fig. 5 a singular point exists. As Ga mole fraction increases, each curve approaches its transi-

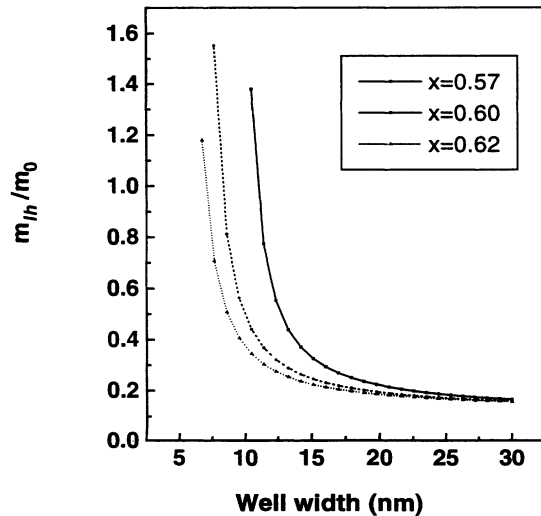


FIG. 4. Light-hole effective masses in a strained quantum well as a function of well widths for different Ga mole fractions for tensile strain cases in  $\text{In}_{1-x}\text{Ga}_x\text{As}/\text{InGaAsP}$  material system.

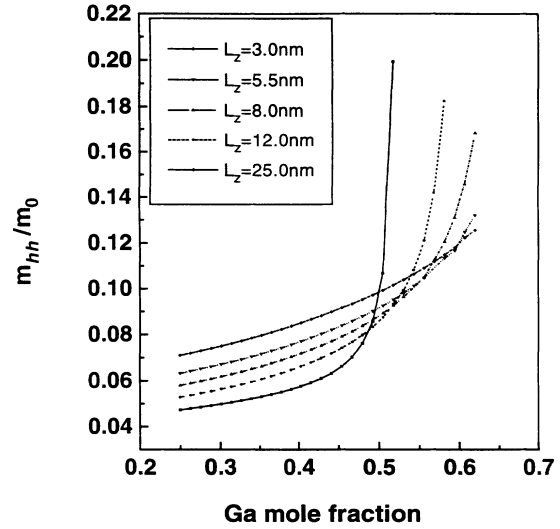


FIG. 5. Heavy-hole effective masses in a strained quantum well as a function of Ga mole fractions for different well widths for  $\text{In}_{1-x}\text{Ga}_x\text{As}/\text{InGaAsP}$  material system.

tion point (see Fig. 3). Heavy-hole effective masses increase to infinity. Figure 6 shows the results of light-hole effective masses in strained quantum well as a function of Ga mole fraction for different well width for  $\text{In}_{1-x}\text{Ga}_x\text{As}/\text{InGaAsP}$  material system. There is a minimum in light-hole effective masses as strain increases, after which, light-hole effective masses increases with tensile strain. In Fig. 6, selected well widths are relatively small because large well width may not be feasible due to the restriction of critical layer thickness.

Band offset is modified due to strain in strained quantum-well structures. Heavy hole and light hole are experiencing different potential barriers. As shown in Fig. 7, the potential for heavy holes vanishes with Ga mole fraction beyond about 0.67 for  $\text{In}_{1-x}\text{Ga}_x\text{As}/\text{InGaAsP}$  quantum-well structures, which

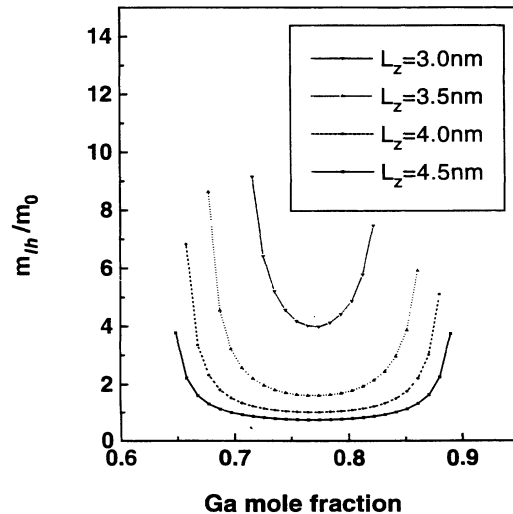


FIG. 6. Heavy-hole effective masses in strained quantum well as a function of Ga mole fraction and well width for tensile strain cases in  $\text{In}_{1-x}\text{Ga}_x\text{As}/\text{InGaAsP}$  material system.

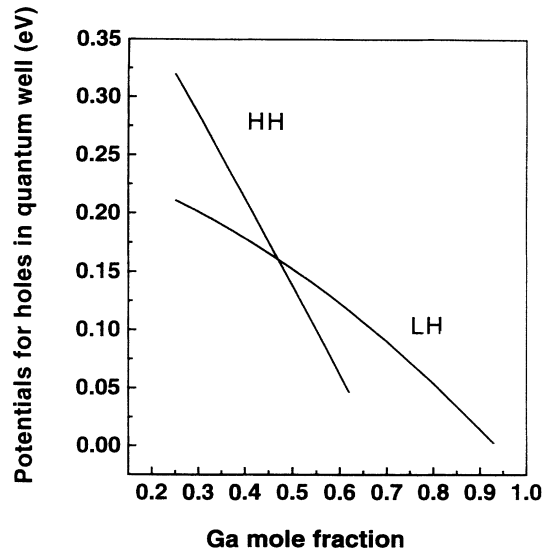


FIG. 7. Valence-band offset for heavy (HH) and light (LH) holes in strained quantum well as a function of Ga mole fraction for  $\text{In}_{1-x}\text{Ga}_x\text{As}/\text{InGaAsP}$  material system.

means no more heavy-hole subbands beyond this point. But light-hole subbands are still possible to about 0.93 in Ga mole fraction, where the potential barrier for light holes also vanishes. This tells us that when Ga mole fraction in  $\text{In}_{1-x}\text{Ga}_x\text{As}/\text{InGaAsP}$  structure is less than about 0.67, both heavy holes and light holes are present;

when Ga mole fraction is between 0.67 and 0.93, only light holes are possible; when Ga mole fraction is above 0.93, no holes are possible.

#### IV. CONCLUSIONS

Hole effective masses, subband levels, and heavy-hole–light-hole splittings are calculated numerically in a large range of material compositions and quantum-well width. Strain Hamiltonian including heavy-hole–light-hole band mixing was utilized in the calculation. A systematic overview of the effective masses, strained quantum-well hole subbands has been provided. Results showed that by adjusting strain and quantum-well width, effective masses, as well as quantum-well subbands, can be effectively modified. This will enable us to engineer quantum-well structures for specific device requirements.

At the present time there is only a limited number of experimental results concerning light- and heavy-hole effective masses in quantum-well structures, with or without strain effects. It is our hope that those theoretical investigations will stimulate experimental efforts in this field.

#### ACKNOWLEDGMENT

The authors would like to acknowledge the financial support of the Natural Sciences and Engineering Research Council of Canada.

<sup>1</sup>E. P. O'Reilly, *Semicond. Sci. Technol.* **4**, 121 (1983).

<sup>2</sup>S. W. Corzine, R.-H. Yan, and L. A. Coldren, in *Quantum Well Lasers*, edited by P. S. Zory, Jr. (Academic, New York, 1993), p. 17.

<sup>3</sup>Eoin P. O'Reilly and Alfred R. Adams, *IEEE J. Quantum Electron.* **30**, 366 (1994).

<sup>4</sup>Doyeol Ahn and Shun Lien Chuang, *IEEE J. Quantum Electron.* **30**, 350 (1994).

<sup>5</sup>B. K. Ridley, *J. Appl. Phys.* **68**, 4667 (1990).

<sup>6</sup>L. Vina, L. Munoz, N. Mestres, E. S. Koteles, A. Ghiti, E. P. O'Reilly, D. C. Bertolet, and K. M. Lau, *Phys. Rev. B* **47**, 13 926 (1993).

<sup>7</sup>Takuya Ishikawa and John E. Bowers, *IEEE J. Quantum Elec-*

*tron.* **30**, 562 (1994).

<sup>8</sup>Ikuo Suemune, *IEEE J. Quantum Electron.* **27**, 1149 (1991).

<sup>9</sup>Doyeol Ahn and Shun-Lien Chung, *IEEE J. Quantum Electron.* **24**, 2400 (1988).

<sup>10</sup>M. G. Burt, *Semicond. Sci. Technol.* **2**, 460 (1987).

<sup>11</sup>M. G. Burt, *Semicond. Sci. Technol.* **3**, 739 (1988).

<sup>12</sup>M. G. Burt, *Semicond. Sci. Technol.* **3**, 1224 (1988).

<sup>13</sup>M. G. Burt, *J. Phys. Condens. Matter* **4**, 6651 (1992).

<sup>14</sup>Johnson Lee and M. O. Vassell, *Phys. Rev. B* **37**, 8855 (1988).

<sup>15</sup>S. L. Chuang, *Phys. Rev. B* **43**, 9649 (1991).

<sup>16</sup>Shun-Lien Chuang, *Phys. Rev. B* **41**, 10 379 (1989).

<sup>17</sup>S. Dubovitsky, A. Mathur, W. H. Steiner, and P. D. Dapkus, *IEEE Photon. Technol. Lett.* **6**, 176 (1994).